J. Marine Sci. Appl. (2013) 12: 251-260
DOI: 10.1007/s11804-013-1196-8

Optimization of Bow Shape for a Non Ballast Water Ship

Ngo Van He* **and Yoshiho Ikeda**

Marine System Engineering, Osaka Prefecture University, Osaka 599-8531, Japan

Abstract: In this research, a commercial CFD code "Fluent" was applied to optimization of bulbous bow shape for a non ballast water ships (NBS). The ship was developed at the Laboratory of the authors in Osaka Prefecture University, Japan. At first, accuracy of the CFD code was validated by comparing the CFD results with experimental results at towing tank of Osaka Prefecture University. In the optimizing process, the resistances acting on ships in calm water and in regular head waves were defined as the object function. Following features of bulbous bow shapes were considered as design parameters: volume of bulbous bow, height of its volume center, angle of bow bottom, and length of bulbous bow. When referring to the computed results given by the CFD like resistance, pressure and wave pattern made by ships in calm water and in waves, an optimal bow shape for ships was discovered by comparing the results in the series of bow shapes. In the computation on waves, the ship is in fully captured condition because shorter waves, λ/L_{pp}<0.6, are assumed.
Keywords: CFD; bulbous bow; non ballast water ships; resistance

Article ID: 1671-9433(2013)03-0251-10

1 Introduction

Non ballast water tankers and bulk carriers were developed at the Laboratory of the authors in Japan. It could be discovered that the ships drastically reduced their resistance in calm water by eliminating large amount of ballast water. The ship has multiple podded propulsors which can move up and down to keep the propeller-depth in non ballast water condition, round cross sections to reduce its wetted surface, a buttock-flow stern shape to reduce its viscous pressure resistance, a frontal engine room to reduce trim angle in non ballast water condition, and a streamlined super-structure to reduce its wind resistance. It was confirmed that the ships could reduce the resistance by 43.7% in ballast condition and by 17.4% in full load condition (Tatsumi *et al*., 2010). At the first stage of the project, a hull form was developed as a hull with a blunt bow and without a bulbous bow, and it is named as the original model (Tatsumi *et al*., 2011; Tomita *et al*., 2011). The resistance tests of the model demonstrated that it has a rather higher resistance in low Froude number even under 0.15 because wave resistance may slightly occur.

It is well known that a bulbous bow which is appropriately designed can reduce the wave resistance by using interference effect of waves generated by the bulbous bow and a main hull (He *et al*., 2012a; He *et al*., 2012b). In this paper, the optimum bulbous bow for the non ballast water ship is determined by using a commercial CFD code "Fluent". In the first part of the paper, validations of the CFD results of the flow around ship hulls and the resistance acting on them in calm water and in regular head waves are carried out by comparing the results with experimental results. It is well known that CFD results depend on calculation domain, number and shape of meshes and turbulent models. A lot of calculations of the CFD in various calculating conditions are carried out, and the results are carefully compared with the experimental results to determine appropriate conditions in the CFD. As the results indicate, accuracy of the CFD is confirmed to be fairly good for the present purposes and that the CFD gives us a lot of information on pressure distributions, wave patterns, and flow fields in boundary layer as well as the total resistance acting on ship hulls.

In the second part of this paper, the CFD was applied to optimize the bow shape in calm water and in regular head waves. On the basis of the calculated results, the optimum bulbous bow shape was developed.

Fig. 1 Non ballast water tanker developed at Ikeda Lab of Osaka Prefecture University, Japan

2 Validation of the used CFD

2.1 Model ships used for validation

Figs. 2 and 3 show the models of the non ballast water ships used for validating the CFD code. One is a simple hull shape without bulbous bow named as "NBS original", and the other one is the improved one, named as "NBK-N6", with a large bulbous bow to reduce the wave resistance in calm water. NBS means non ballast water ship and NBK means non ballast water tankers and bulkers which were developed at Ikeda's Lab. These ships have the same stern shape but different bow shapes. Table 1 shows the principal particulars of them.

Received date: 2013-04-16.
Accepted date: 2013-06-04.
***Corresponding author Email:** nvhe_bk@yahoo.com

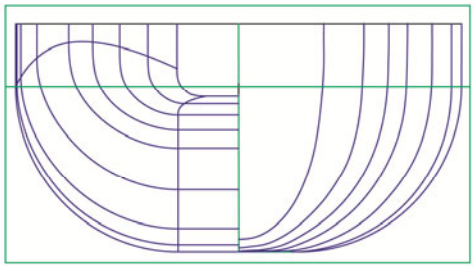

Fig. 2 Body plan of the simple hull form, named as NBS−original, without bulbous bow

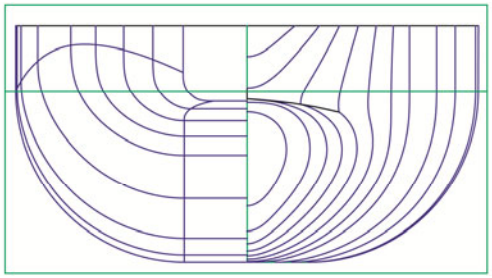

Fig. 3 Body plan of the improved hull form, NBK-N6 with a developed bulbous bow to reduce the wave resistance in calm water

Table 1 Principal particular of two models

Items	NBS-original	NBK-N6
Length, L_{pp}/m	2.000	2.000
Breadth, B/m	0.359	0.355
Draft/m	0.131	0.131
Displacement, Dispt/t	0.065 04	0.063 88
Wetted surface area, WSA/m^2	0.921	0.925

2.2 Assessment of CFD results in calm water

Accuracy of the CFD results of resistances was validated by comparing the results with experimental results obtained at the towing tank of Osaka Prefecture University.

In computation, a commercial CFD code "Fluent" was used. The volume of fluid (VOF) model k-ω for unsteady flow was used. The velocity inlet is set up for the inlet. The pressure outlet is setup for the outlet of the fluid domain for calculation. Structured H–grid is used for meshing of 1.8 million grids (He *et al*., 2011).

In Fig. 4, the frictional resistances acting on the hulls of these ships obtained by Schoenherr's formula and the CFD code are compared. Slight difference between them can be seen.

Fig. 5 shows the comparison between calculated and experimental results of the total resistance acting on the ships in calm water. The agreement between calculated and experimental results was fairly good.

The computed and measured velocity distributions in boundary layers at stern part are compared in Fig. 6. The agreement between them is fairly good, and we can say that viscous forces are obtained in good accuracy by the CFD code.

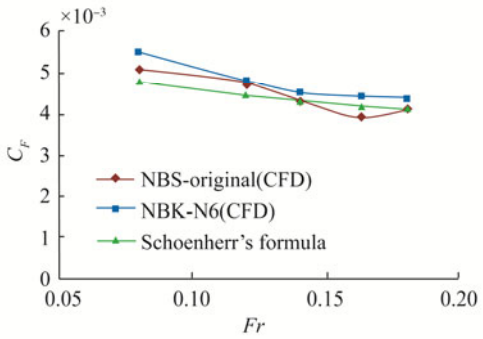

Fig. 4 Frictional resistances calculated by Schoenherr's formula and CFD

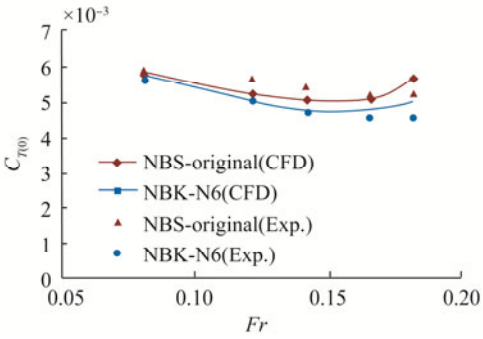

Fig. 5 Total resistances obtained by CFD and experiments

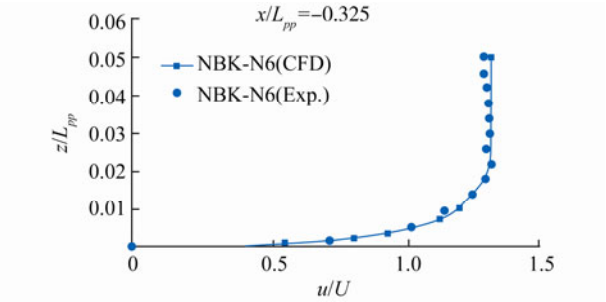

Fig. 6 Velocity distribution in boundary layer at centerline of x/L_{pp}=−0.325, Fr=0.163 in calm water

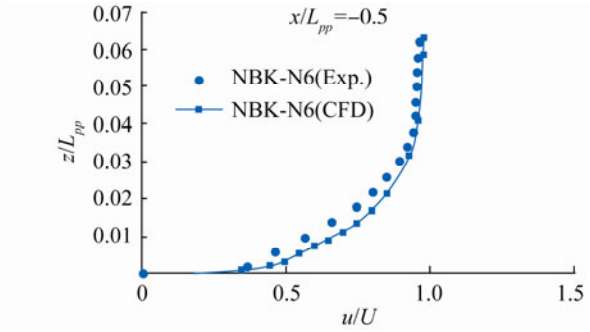

Fig. 7 Velocity distribution in boundary layer at centerline of AP; x/L_{pp}=−0.5, at Fr=0.163 in calm water

In Fig. 7, the velocity distributions in boundary layer at after perpendicular (AP) of the ship obtained by the experiments and the CFD computations are compared. The agreement between them becomes a little worse compared with results from Fig. 6.

2.3 Assessment of CFD results in regular waves

In this section, accuracy of the calculated results by the CFD code in regular head waves will be assessed by comparing the calculated results for the two models with experimental results measured by the authors. The incident waves are shorter than the regular heads (λ/L_{pp}<0.6) and the wave height is H_w=0.02 m for 2 m models. The Froude number is 0.163. In this research, CFD computation was completed using an unsteady flow.

In Figs. 8 and 9, the calculated and experimental results of resistance are shown as the ratio of resistance coefficient of NBK-N6 to that of the NBS-original model. The results show that agreement between CFD results and experimental results of total resistance of the ships in regular head waves is fairly good. Added resistance acting on NBK-N6 in regular waves decreases by 25% due to the developed bulbous bow.

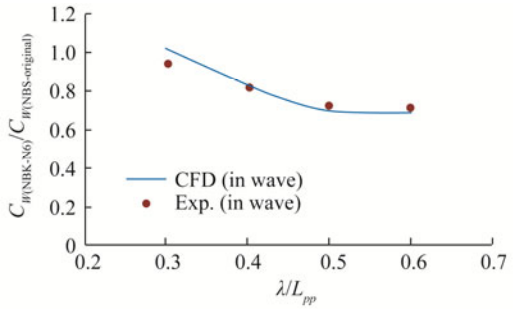

Fig. 8 Ratio of added resistances of two ships in regular head waves, H_w=0.02 m at Fr=0.163

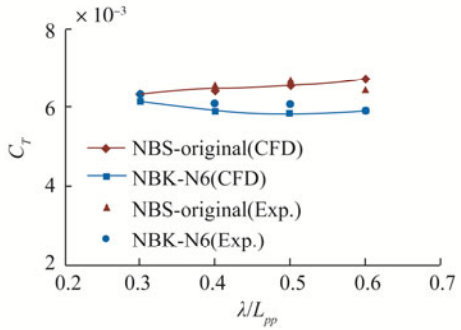

Fig. 9 Total resistance coefficients of two ships in regular head waves, H_w=0.02 m at Fr=0.163

3 Optimization of bulbous bow shape

3.1 Design parameters of optimum bulbous bow shape

In this section, the commercial CFD 'Fluent' was applied to optimization of the bulbous-bow shape of the non ballast-water ship. The resistance acting on the ship in calm water and in regular head waves is defined as the object function in the optimization process. Following features of bulbous bow shapes are considered as design parameters: volume of bulbous bow, height of volume center, angle of bow bottom, and length of bulbous bow.

3.1.1 Volume of bulbous bow

In this optimizing process, the original ship with a blunt simple bow shape, NBS-original, which was first developed in the research project to develop a non ballast water ships was selected as the initial model. The NBS-original has some wave resistance in low Froude number, and a bulbous bow is needed to reduce the wave resistance. An optimum bulbous bow shape for the ship was developed in the optimizing process by using the CFD. The stern of all ships is the same as that of the NBS-original. The length, breadth and draft of the ships keep the same. The volume of the ships was slightly changed from that of NBS-original.

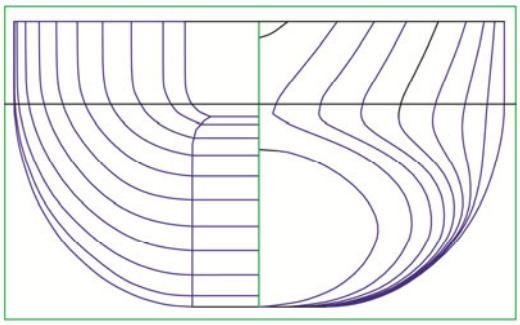

Fig. 10 Body plan of a new ship with developed bulbous bow shape, NBK-N1

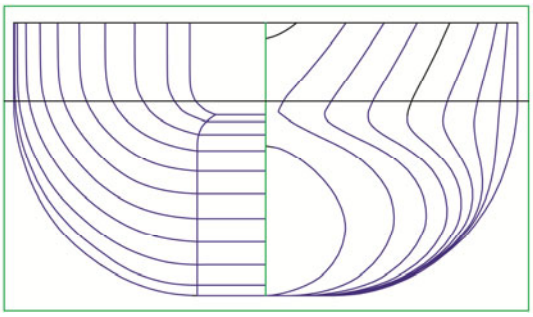

(a) NBK-N2

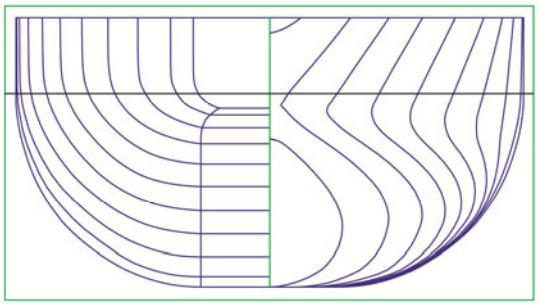

(b) NBK-N3

Fig. 11 Body plans of new ships with developed bulbous bow shapes, NBK-N2 & NBK-N3

Table 2 Principal particulars of models

No	L_{pp}/m	B/m	Draft/m	Dispt/t	WSA/m^2
NBK-N1	1.998	0.355	0.129	0.064 45	0.962 6
NBK-N2	1.998	0.355	0.130	0.064 43	0.953 9
NBK-N3	1.999	0.355	0.131	0.064 69	0.953 9

Figs. 10 and 11 show the body plans of the newly developed ships. The principal particulars of them are shown in Table 2. The resistances acting on them are calculated by using the CFD. Calculated total resistances acting on them running in calm water and in regular head waves are shown in Figs. 12 and 13. In the calculation on waves, the ship is in fully captured condition of waves because the wave length is assumed to be short compared with ship length and ship motions can be neglected.

The results shown in Fig. 12 demonstrate that the bulbous bow of NBK-N1 is too large to decrease the wave resistance and NBK-N3 has the minimum resistance among them in calm water.

The results on waves shown in Fig. 13 demonstrate that NBK-N3 has the minimum resistance in shorter waves, λ/L_{PP}=0.3 and 0.4, but NBK-N2 has smaller resistance than NBK-N3 if λ/L_{PP}=0.5 and 0.6. The results suggest that the optimum bulbous bow depends on wave length of encounter waves.

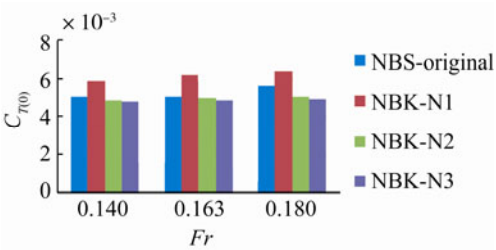

Fig. 12 Calculated total resistances of new ships in calm water

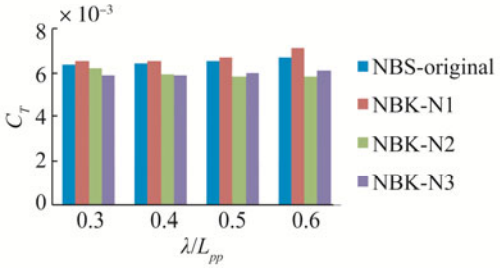

Fig. 13 Calculated results of total resistances of the ships in regular head waves at Fr=0.163; H_w=0.02 m

3.1.2 Height of volume center and angle of bow bottom

In the next step, the height of volume center of the bulbous bow and angle of bow bottom line of the ships were changed from low to high as shown in Fig. 14. The NBK-N3 is the best one in case of optimum volume of bow shape in calm water as shown in previous section. Table 3 shows their principal particulars.

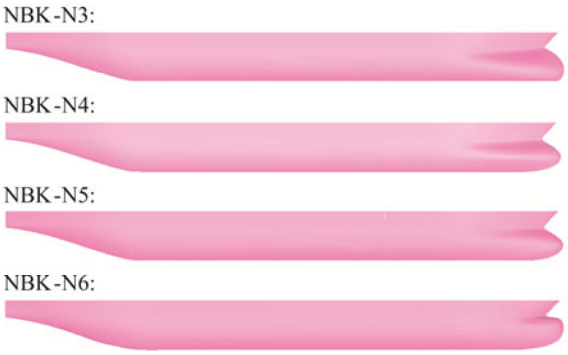

Fig. 14 Side profiles of newly developed ships with different height of volume center and angle of bow bottom line

Table 3 Principal particulars of models

No	L_{pp}/m	B/m	Draft/m	Dispt/t	WSA/m^2
NBK-N4	1.999	0.355	0.131	0.063 76	0.938 3
NBK-N5	2.000	0.355	0.134	0.064 55	0.931 7
NBK-N6	2.000	0.355	0.131	0.063 88	0.925 0

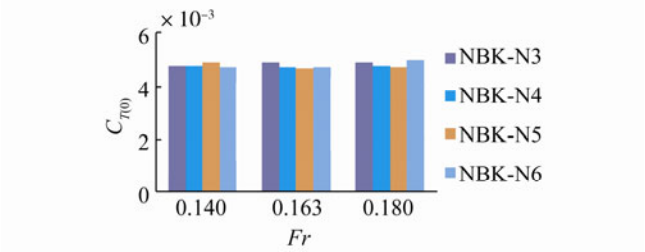

Fig. 15 Calculated total resistances of new ships in calm water

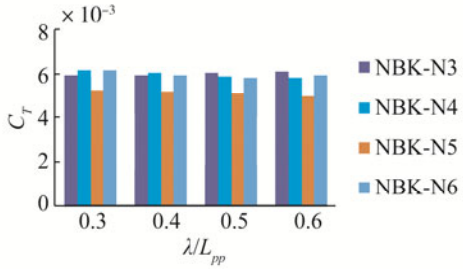

Fig. 16 Calculated results of total resistances of the ships in regular head waves at Fr=0.163; H_w=0.02 m

Figs. 15 and 16 show the calculated results of resistances acting on them in calm water and in regular head waves. The calculated results of resistances in calm water shown in Fig.15 show that at Froude number 0.14 NBK-N6 is the best one, and at Froude number 0.16, 0.18 NBK-N5 is the best one. The optimum bow shape depends on Froude number.

In regular head waves, NBK-N5 has the minimum resistance in wave height H_w of 0.02 m and in the region of λ/L_{pp}<0.6 as shown in Fig. 16.

3.1.3 Length of bow

In the next step, length of bow of NBK-N5, which is the minimum resistance hull form in previous optimum process, is changed. The volume of each newly developed ship keeps the same as that of NBK-N5. Fig. 17 shows the profiles on center planes of bows of them and their principal particulars are shown in Table 4.

Figs. 18–20 show the calculated results of resistance acting on the newly developed ships in calm water and in regular head waves. The calculated results show that model named as NBK-N5 is the minimum resistance hull form in calm water and in regular head wave in this series of ships.

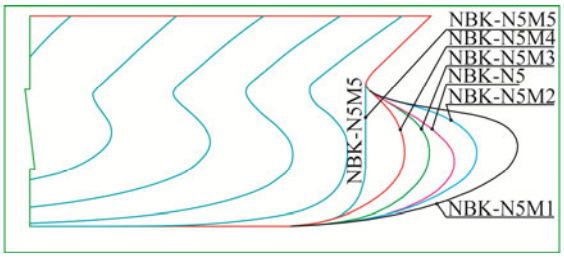

Fig. 17 Profiles of bow of newly developed ships

Table 4 Principal particulars of models

No	L_{pp}/m	B/m	Draft/m	Dispt/t	WSA/m^2
NBK-N5M5	2.083	0.371	0.128	0.065 04	0.944 5
NBK-N5M4	2.080	0.370	0.128	0.065 04	0.949 7
NBK-N5M3	2.078	0.369	0.128	0.065 04	0.953 5
NBK-N5M2	2.075	0.369	0.127	0.065 04	0.961 6
NBK-N5M1	2.073	0.368	0.127	0.065 04	0.968 6

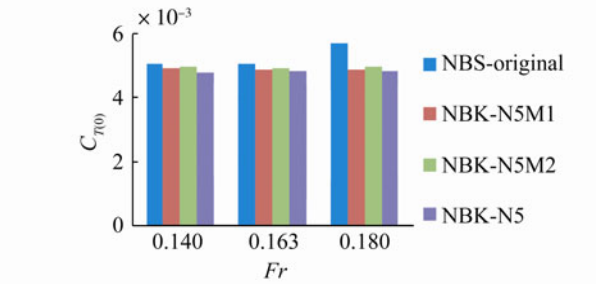

Fig. 18 Calculated total resistances of new ships in calm water; NBK-N5M1, NBK-N5M2

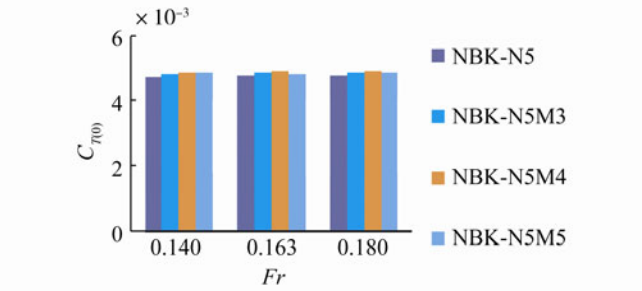

Fig. 19 Calculated total resistances of new ships in calm water; NBK-N5M3, NBK-N5M4 and NBK-N5M5

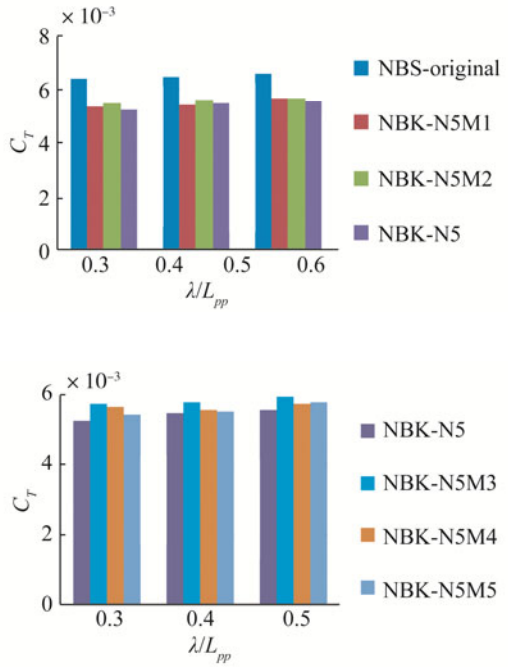

Fig. 20 Calculated total resistances in regular head waves, H_w=0.02 m at Fr=0.163

4 Assessment of effects of bulbous bow

In this section assessment of the effects of bulbous bows will be discussed to understand the causes of reducing resistance by an appropriately designed bulbous bow.

4.1 Assessment of effects of bulbous bow on reducing resistance acting on ships in calm water

Computed results of two ships, the model NBS-original without bulbous bow and NBK-N6 with a developed bulbous bow are compared in this section.

Fig. 21 shows reduction of the pressure resistance of NBK-N6 from that of the NBS-original model. In the pressure resistance, wave and viscous pressure resistances are included. We can see that the pressure resistance decreases due to the bulbous bow of NBK-N6 with increasing advanced speed and is smaller by 70% than that of NBS-original at Froude number of 0.15. In the figure the experimental results of residual resistance component are also shown. The agreement between them is fairly good.

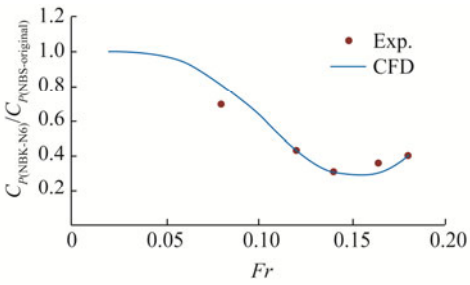

Fig. 21 Ratio of pressure resistances coefficient of NBK-N6 to that of NBS-original in calm water

The computed results of dynamic pressure distribution over front-half hull surface and wave pattern around the hulls of the two ships running in calm water are shown in Figs. 22 and 23. The dynamic pressure is at just outside of boundary layer. These results give us some important information for understanding the reasons why the bow shape reduces resistances acting on a ship in calm water and in waves.

The calculated dynamic pressure distributions shown in Fig. 22 demonstrate that wide and low dynamic pressure area (blue area) over the front-edge of bow of NBS-original disappears on the bow of NBK-N6 with the bulbous bow. Since low dynamic pressure causes high pressure over the hull surface, the resistance acting on the hull must increase if the area of low dynamic pressure area is wide. On the contrary, lower dynamic pressure (Red or yellow area in the figures) reduces the resistance. From these dynamic pressure distributions, we can imagine how the bulbous bows change the flow around the hulls and the pressure over the hull surface.

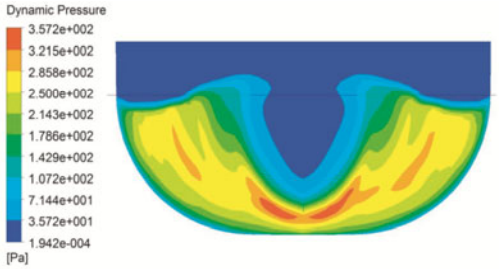

(a) NBS-original

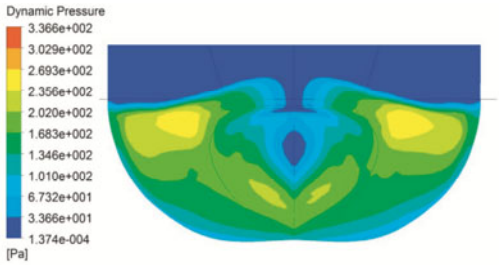

(b) NBK-N6

Fig. 22 Dynamic pressure distributions over front-half hull surface of ships at *Fr*=0.163 in calm water

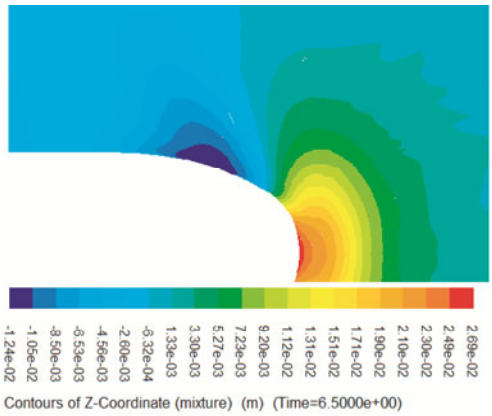

(a) NBS-original

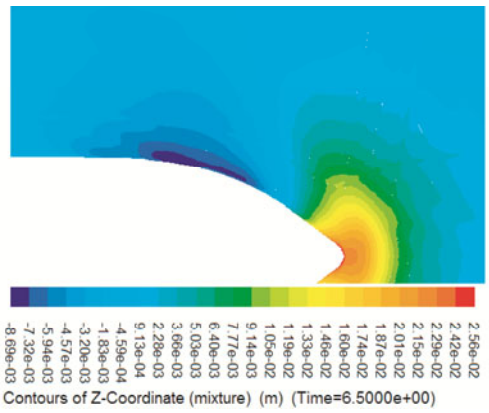

(b) NBK-N6

Fig. 23 Calculated wave patterns on free surface around ships at *Fr*=0.163 in calm water

(a) NBS-original

(b) NBK-N6

Fig. 24 Wave patterns near bows of ships at *Fr*=0.163 in calm water

Fig. 23 shows the calculated free-surface levels around the bows of NBK-N6 and NBS-original. The results demonstrate higher and wider waves are created in front of the bow of NBS-original than that of NBK-N6. It can be seen that the waves near shoulder are also different. In Fig. 24 photographs of bow waves of NBK-N6 and NBS-original which are taken in a circulating water channel are shown. Similar wave patterns to the calculated results obtained by the CFD can be seen in the experimental photographs.

In Figs. 25 and 26 calculated wave profiles in front of the bows of NBK-N6 and NBS-original are shown. In the figures, x denotes longitudinal axis, where plus of the x axis is defined from aft to front of the ship, the origin of which is at the mid-ship. y is transverse axis, the origin of which, y=0 is located in the centerline of the ship and z is vertical axis,

zero is set at the draft of the ship, where plus of z is defined from the bottom to upper direction. The results demonstrate that generated waves in calm water are significantly reduced by the newly developed bulbous bow of NBK-N6.

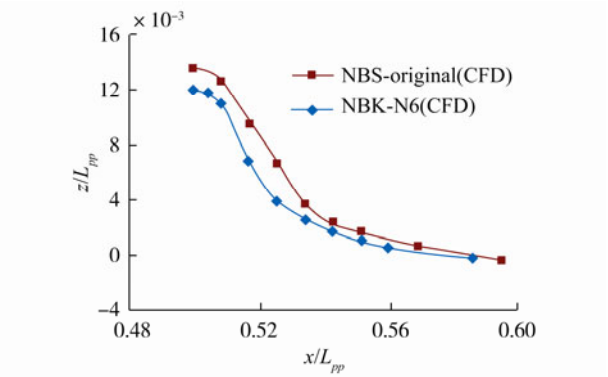

Fig. 25 Profile of waves generated by ships at y/B=0, Fr=0.163 in calm water

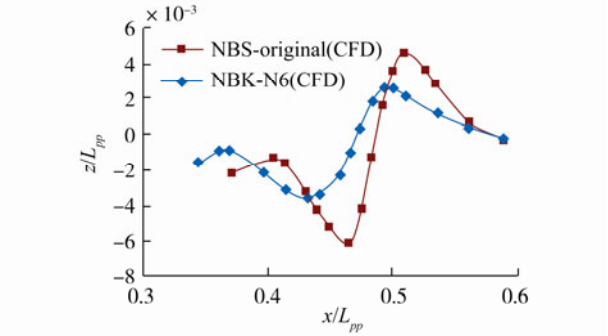

Fig. 26 Profile of waves generated by ships at y/B=0.5, Fr=0.163 in calm water

4.2 Assessment of effect of bulbous bow on added resistance acting on ships in waves

In this section, assessment of the effect of bulbous bows on added resistance acting on ships in regular head waves is discussed to find reasons why the added resistance due to waves depends on bow shapes. Pressure distribution over hull surface of ships and wave patterns generated by the ships moving in waves are computed by the CFD.

4.2.1 Pressure distribution and wave pattern

Fig. 27 shows the computed dynamic pressure distributions over the front−half surface of the hulls running in regular head waves; H_w=0.02 m, λ/L_{pp}=0.3 at Fr=0.163. The results at the same phase in waves are shown.

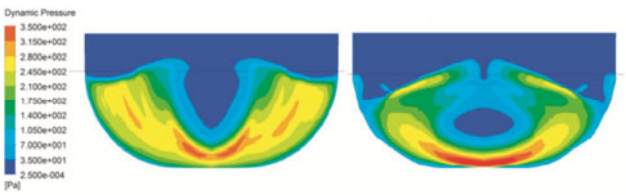

NBS-original NBK-N1

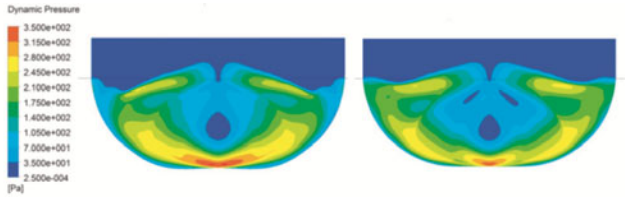

NBK-N2 NBK-N3

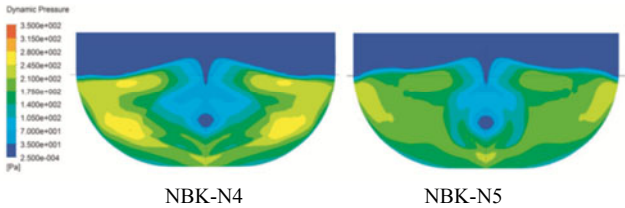

NBK-N4 NBK-N5

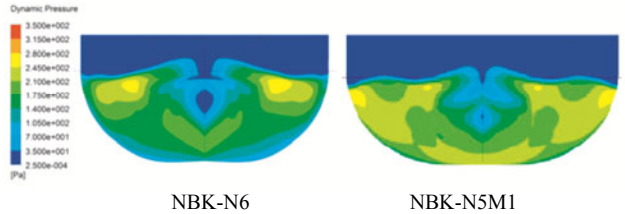

NBK-N6 NBK-N5M1

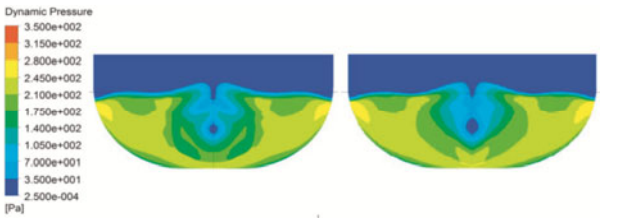

NBK-N5M2 NBK-N5M3

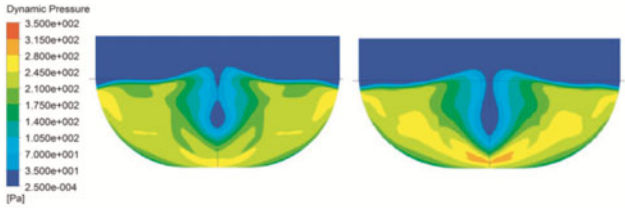

NBK-N5M4 NBK-N5M5

Fig. 27 Dynamic pressure distributions on front-half hull surface of developed ships at the same phase in regular head waves, H_w=0.02 m, λ/L_{pp}=0.3 at Fr=0.163

Fig. 27 clearly shows difference of pressure over half-front surface of the hulls with newly developed bow shapes. The area where is in lower dynamic pressure (blue area in the figure) is in higher static pressure acting on the hull surface. This means that smaller high pressure area induces higher added resistance. The results demonstrate that the newly developed bow shapes may reduce the resistance.

Figs. 28 and 29 show the computed wave patterns on free surface around the ships running in regular head waves; H_w=0.02 m, λ/L_{pp}=0.3 at Froude number of 0.163.

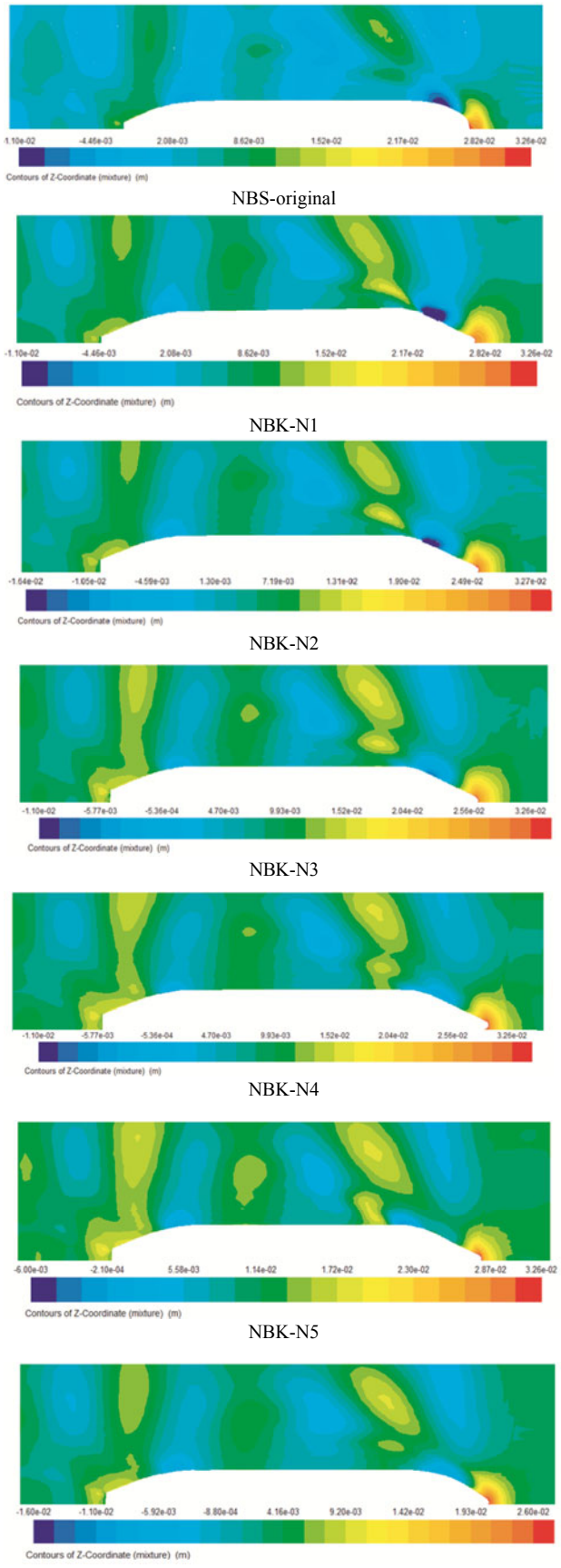

Fig. 28 Waves patterns on free surface in regular head waves, H_w=0.02 m, λ/L_{pp}=0.3 at Fr=0.163

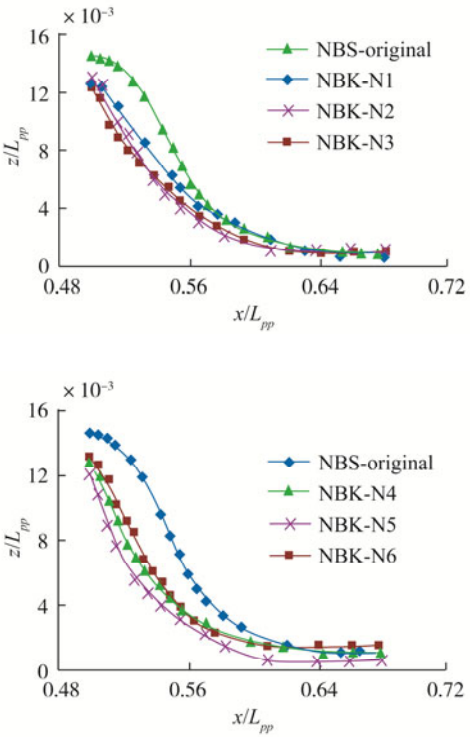

Fig. 29 Wave profiles on free surface near bow at y/B=0, in regular head waves, H_w=0.02 m, λ/L_{pp}=0.3 at Fr=0.163

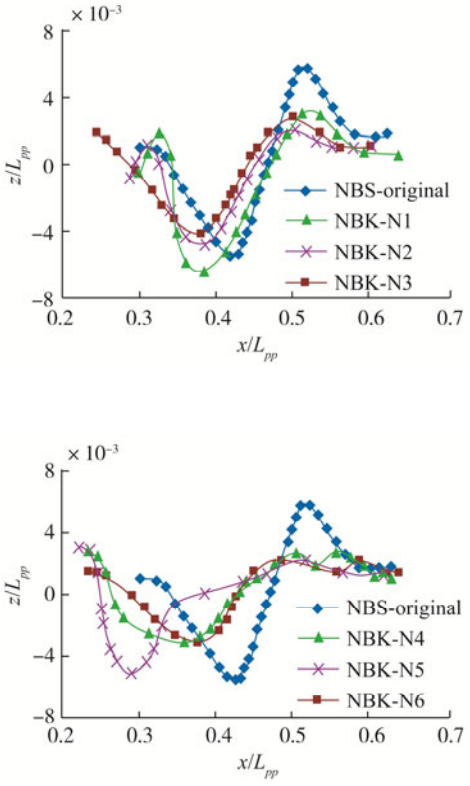

Fig. 30 Wave profiles on free surface near bow at y/B= 0.5, in waves, H_w=0.02 m, λ/L_{pp}=0.3 at Fr=0.163

Figs. 29 and 30 show the calculated profiles of wave on free surface near the bows of the ships.

Figs. 28–30 clearly show that generated waves by the ships in waves on free surface depend on the developed bow shapes and decrease by the bulbous bow compared with those of the original model. The results may suggest that the added resistance of the newly developed hull forms decrease in regular head waves.

4.2.2 Added resistance acting on new ships in waves

In this section, added resistances acting on the hull of the new ships in waves are computed. The results are compared with each other to find the minimum added resistance hull form.

Fig. 31 shows the computed added resistances of the ships in waves with wave height: H_w= 0.02 m and at Fr=0.163. The added resistance coefficient is defined as follows:

$$C_W = C_{T(W)} - C_{T(O)} \quad (1)$$

where $C_{T(W)}$ and $C_{T(O)}$ are the coefficients of resistance in waves and in calm water, respectively.

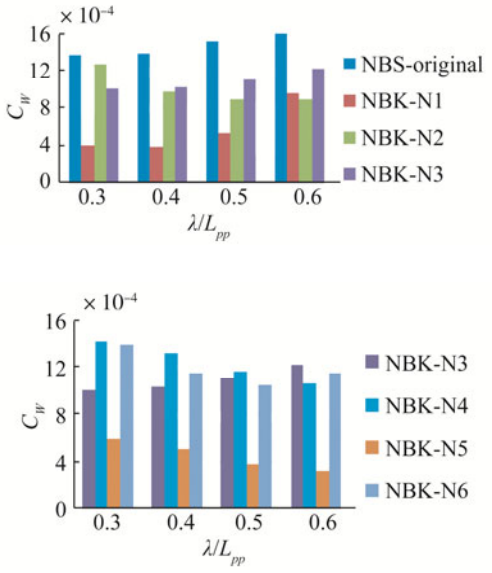

Fig. 31 Calculated results of added resistances in waves with H_w=0.02 m and at Fr=0.163

These results show that the ships with developed bulbous bows have smaller added resistance than that of NBS-original. The results also demonstrate that the added resistances acting on ships depend on wave length. At λ/L_{pp}<0.4, NBK-N1 with a larger bulbous bow has the minimum added resistance, at λ/L_{pp}>0.4, NBK-N5 has the minimum added resistance.

In the computed results, we can see different characteristics of the added resistance in waves. The added resistances due to waves acting on NBK-N1 and NBK-N3 with larger bulbous bow and on NBS-original with a blunt bow increase with the increased wave length. On the contrary, the added resistances acting on hulls with smaller bows like NBK-N4, NBK-N5 and NBK-N6 decrease with the increased wave length, as shown in Fig. 31.

5 Conclusions

In this paper, by using the commercial CFD "Fluent", an optimum bulbous bow for a non ballast water ship in calm water and in regular head waves was developed, and the following conclusions were obtained:

1) It was confirmed that a commercial CFD code "Fluent" provides fairly good results of the resistance acting on a ship hull both in calm water and in regular head waves with H_w=0.02 m; λ/L_{pp}<0.6, and viscous flow in boundary layer around it in calm water.

2) A series of bow shapes which reduce the resistance in waves as well as in calm water were developed and the resistances of the series of hulls were then calculated by the CFD to find an optimum hull shape. The optimum bow shapes among the developed hulls were determined by comparing the calculated resistances for the series of hulls.

3) In the evaluation of the total resistance acting on hulls of ships, the optimum hull shape depends on Froude number.

4) The obtained optimum hull shape can decrease the resistance in regular head waves by 25% at λ/L_{pp}<0.6.

5) The CFD gives us many calculated results like pressure distributions on the hull surface, wave patterns on free surface, and so on. The information plays an important role for understanding the phenomenon which causes the added resistance due to waves.

References

He NV, Nihei Y, Ikeda Y (2012a). A study on application of a commercial CFD code to reduce resistance acting on a NBT-Part 1. *The Japan Society of Naval Architects and Ocean Engineers*, Kobe, 415-418.

He NV, Nihei Y, Ikeda Y (2012b). A study on application of CFD code to reduce resistance acting on a non ballast tanker-Part 2. *The 6th Asia-Pacific Workshop on Marine Hydrodynamic*, Johor, 264-269.

He NV, Nihei Y, Ikeda Y (2012c). A study on an optimum hull form in waves for a non ballast tankers and bulkers. *The Advanced Maritime Engineering Conference and the 5th Pan Asian Association of Maritime Engineering Societies*, Taipei, Paper No. NSC-01.

Tatsumi T, Nihei Y, Ikeda Y (2010). Development of a new energy saving tanker with non ballast water and podded propulsor. *The 5th Asia-Pacific Workshop on Marine Hydrodynamic*, Osaka, 25-28.

Tatsumi T, Nihei Y, Ikeda Y (2011). Development of a new energy saving tanker with non ballast water-Part 1. *The Japan Society of Naval Architects and Ocean Engineers,* Fukuoka, 216-218 (in Japanese).

Tomita A, Nihei Y, Ikeda Y (2011). Development of a new energy saving tanker with non ballast water-Part 2. *The Japan Society of Naval Architects and Ocean Engineers*, Fukuoka, 219-222 (in Japanese).

Author biographies

Ngo Van He is a PhD student at Ikeda Laboratory of Osaka Prefecture University, Japan. He studies on CFD application, developing hull form for a non ballast water ships and hydrodynamic performance of ships.

Yoshiho Ikeda is a professor in Marine System Engineering of Osaka Prefecture University, Japan. His current research project is developing non ballast water ships. He is interested in next generation innovative ships, hydrodynamic of ships, economics of cruise ships.

33rd International Conference on Ocean, Offshore and Arctic Engineering (OMAE2014)

San Francisco, California, June 8-13, 2014

OMAE 2014 is the ideal forum for researchers, engineers, managers, technicians and students from the scientific and industrial communities from around the world to

- meet and present advances in technology and its scientific support;
- to exchange ideas and experiences whilst promoting technological progress and its application in industry
- to promote international cooperation in ocean, offshore and arctic engineering.

Technical Program

Our program will follow the tradition of excellence standard in all previous OMAE conferences. The following 10 standard symposia plus 2 special symposia are planned:

- SYMP 1 Offshore Technology
- SYMP 2 Structures, Safety and Reliability
- SYMP 3 Materials Technology
- SYMP 4 Pipeline and Riser Technology
- SYMP 5 Ocean Space Utilization
- SYMP 6 Ocean Engineering
- SYMP 7 Polar and Arctic Science and Technology
- SYMP 8 CFD and VIV
- SYMP 9 Ocean Renewable Energy
- SYMP 10 Offshore Geotechnics
- SYMP 11 Petroleum Technology
- SYMP 12 Professor Emeritus J. Randolph Paulling Honoring Symposium

Abstract Submission

Authors should submit a 400-word text-only abstract through the OMAE2014 website. For assistance with submitting your abstract online, please view the author help manual.